

Morphology and Temperature Phase Transitions in α,ω -Alkanediols with Different Chain Lengths

Vyacheslav Marikhin,^{*1} Victor Egorov,¹ Elena Ivan'kova,¹ Liubov Myasnikova,¹

Elena Radovanova,¹ Boris Volchek,² Darya Medvedeva,² Alan Jonas³

¹Ioffe Physico-Technical Institute of RAS, Polytekhnicheskaya 26, St. Petersburg 194021, Russia

E-mail: v.marikhin@mail.ioffe.ru

²Institute of Macromolecular Compounds of RAS, Bolshoy pr. V.O. 31, St. Petersburg 199004, Russia

³Universite Catholique de Louvain, Place Croix du Sud, 1B-1348 Louvain-la-Neuve, Belgium

Summary: A comparative analysis of phase transitions in diols with various chain lengths $[(CH_2)_{44}(OH)_2$ and $(CH_2)_{22}(OH)_2]$ and changes in their absorption spectra with temperature have been investigated by DSC and FTIR. Analysis of the DSC data has led to the conclusion that the low-temperature phase transition of $(CH_2)_{22}(OH)_2$ in a solid state ($T_{s-s} = 367.1$ K) is a phase transition of the first order, while the high-temperature phase transition ($T_m = 376.3$ K) is of the second order, i.e., a transition of the order-disorder type. Splitting of the IR absorption bands into doublets at $720\text{--}730\text{ cm}^{-1}$ and $1463\text{--}1473\text{ cm}^{-1}$ indicates that crystalline subcells in the lamellae of both diols are orthorhombic lattices with the parameters typical of hydrocarbons. IR spectra showed that at the phase transition temperature T_{s-s} transformation of an orthorhombic subcell into a hexagonal one occurs. This type of molecular chain packing remains the same up to the melting temperature T_m . In a $(CH_2)_{44}(OH)_2$ diol, the ortho-hexagonal subcell transition occurs only at the melting temperature (390.0 K). The wide IR band in the region from 3000 cm^{-1} to 3600 cm^{-1} shows that end hydroxyl groups of diol molecules form, on the surfaces of lamellar crystals, long (polymer) regular sequences consisting of intermolecular hydrogen bonds.

Keywords: α,ω -alkanediols; DSC; FT-IR; morphology; phase behavior

Introduction

Due to their monodisperse molecular mass and absence of chemical defects, long-chain molecular crystals are suitable models aimed at solving many of the controversial problems concerning the relationship between structure and physical and chemical properties of polymers crystals, such as

the influence of chain length and types of end groups on structure formation during crystallization from solutions and melts, structural and conformational transformations at phase transitions, the nature and energy of generation of conformational and translational defects, etc. Particular advantages of long-chain molecular crystals over conventional polydisperse polymers with chemical defects are offered in establishing general quantitative relationships between structure and different properties of materials.

The simplest long-chain molecular crystals are *n*-paraffins, but even their structure and properties are rather complicated and depend on the number (*n*) of CH₂ groups in the methylene sequence. In addition, the properties of *n*-paraffins depend on whether *n* is odd or even^[1-15]. The structure and properties of long-chain α,ω -alkanediols have not been extensively studied as the paraffins have.^[16-23] The α,ω -alkanediols are particularly attractive because they allow elucidation of the influence of the type of end groups on the structure and properties of diol crystals in comparison with *n*-paraffins with the same chain length (the methylene parts of both compounds contain repeating CH₂ units). Interest in diols is also due to the fact that end hydroxyl groups on basal planes of lamellar crystals form long “polymer” chains consisting of hydrogen bonds. This leads to a significant increase in the surface energy of these crystals and, as a consequence, to changes in their thermodynamical characteristics, such as melting temperature, specific features of phase transitions in the heating-cooling cycles, etc.^[16-23]

The goal of our work was to study the morphology of diols and its transformation at temperature phase transitions in diols which have the chain lengths differing by a factor of two, i.e., 1,22-docosanediol (D-22) and 1,44-tetratetracontanediol (D-44).

Experimental

Materials

The compounds studied were 1,22-docosanediol (D-22) and 1,44-tetratetracontanediol (D-44), synthesized in the laboratory of Prof. A. Jonas (Belgium) from commercially available reagents. D-22 was synthesized using a procedure that was a slight modification of that described in^[23]. D-22 and was recrystallized from methanol. D-44 was synthesized from D-22 by using the same

improved procedure as for D-22. The final product was purified by recrystallization from benzene and discoloration with silica.

Instrumentation

Morphology of the samples was investigated by a JEOL-6300 scanning microscope. A Perkin-Elmer DSC-2 was used for calorimetry studies. Conventional procedures were employed for device calibration. The velocity of scanning V of the thermal flow was varied from $V = 1.25 \text{ K}\cdot\text{min}^{-1}$ to $V = 10 \text{ K}\cdot\text{min}^{-1}$. IR absorption spectra, from room temperature to the melting temperatures of the samples, were recorded by a Bruker JFS-88 (Bruker Analytik GmbH, Rheinstetten, Germany) Fourier spectrometer over a wide range of frequencies, from 500 cm^{-1} to 5000 cm^{-1} .

Results and Discussion

Scanning Electron Microscopy (SEM)

Figures 1 and 2 show scanning electron micrographs of morphological units of the lamellar type arising in the products of synthesis during polymerization-crystallization.

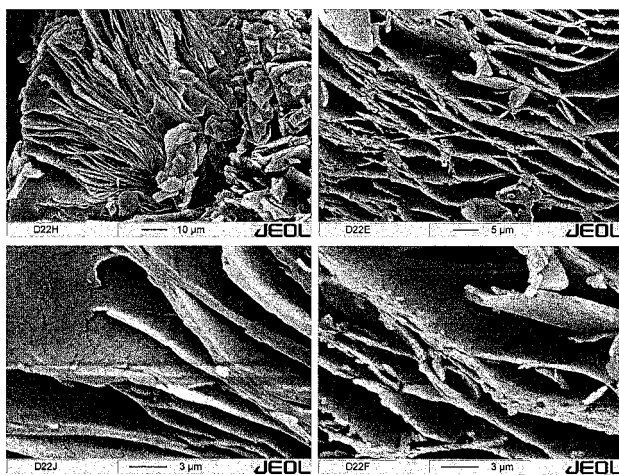


Figure 1. Scanning electron micrographs of 1,22 – Docosanediol.

It can be seen that both types of diols are characterized by formation of fairly long (tens of microns) structures of the lamellar type whose thickness can be as large as units of microns. A tendency toward formation of spherulite-like units is more pronounced in D-22 than in D-44 (Figure 1).

It is known^[24-29] that long-chain molecules in molecular crystals form single lamellae from fully extended chains whose monodisperse thickness is proportional to the molecule length, i.e., it amounts to several tens of nanometers. Therefore, it can be concluded that lamellar structures seen on SEM micrographs (Figures 1 and 2) consist of stacks of several hundreds-thousands of single-crystal lamellae. It has been shown^[17, 18] that in diols with an even number of CH₂ groups the chains are tilted at an angle (30-35°) to the normal to the basal planes formed by end hydroxyl groups. In addition, when lamellae are superposed on each other, the tilts of the angles in neighboring lamellae change to the opposite ones, and, as a consequence, structures of the herring-bone motif arise.^[18, 19]

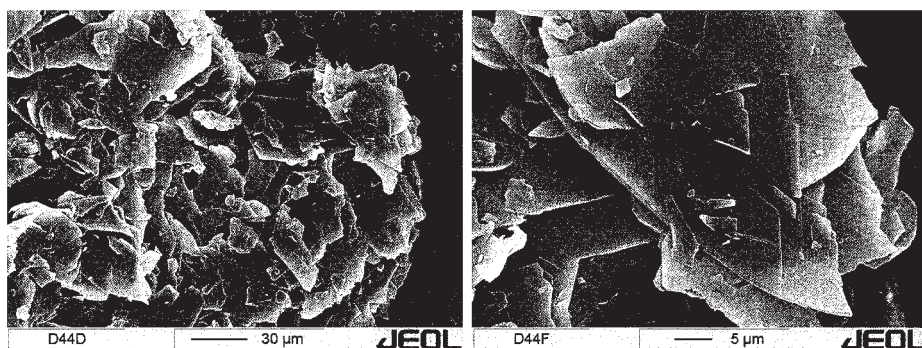


Figure 2. Scanning electron micrographs of 1,44 – Tetratetracontanediol.

Differential Scanning Calorimetry (DSC)

It has been found^[16,19] that in diols, like in n-paraffins, phase transitions are observed, even in the solid state. Their number depends on the chain length and on whether the number of carbon

atoms in the molecule backbone is odd or even.

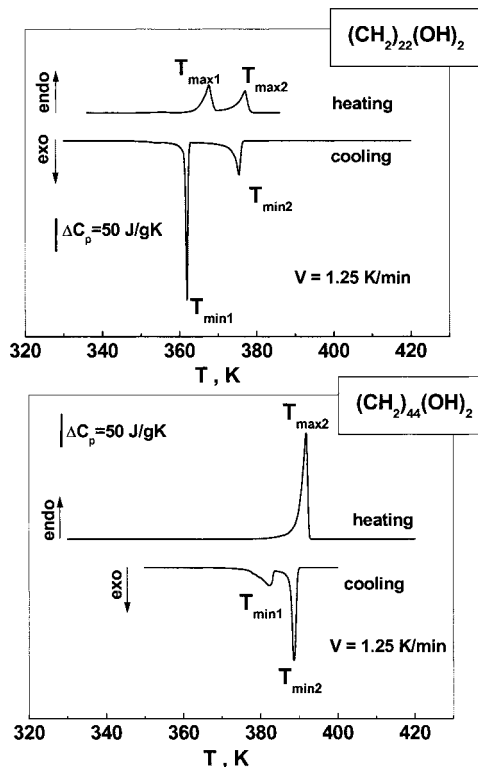


Figure 3. Heating – cooling DSC thermographs of α,ω -alkanediols.

Figure 3 presents the DSC thermograms obtained for the D-22 and D-44 samples with a mass of about 3 mg in the heating-cooling regime. The scanning velocity was $V = 1.25 \text{ K} \cdot \text{min}^{-1}$. It is evident from Figure 3 that the thermogram of the D-22 sample heated from room temperature exhibits an endothermic maximum at T_{max1} (about 367 K), which is attributable to a phase transition in the solid state T_{s-s} . At T_{max2} (in the vicinity of 377 K), melting of the sample takes place (order-disorder transition). When the sample is cooled from the melt, it crystallizes at T_{min2} (disorder-order transition). Further cooling is accompanied by a pronounced exothermal effect,

attributable to the phase transition in the solid state at $T_{\min 1}$. In contrast to D-22, when D-44 is heated, transition from the low-temperature crystalline state into the melt occurs in one stage at the melting temperature $T_{\max 2}$ (in the vicinity of 392 K). No transition of the T_{s-s} type was observed for this sample in the heating cycle. On the other hand, for the D-44 sample cooled from the melt, the second endothermic peak at $T_{\min 1}$ attributable to phase transition in the solid state is observed in addition to the exothermic peak at $T_{\min 2}$ caused by crystallization. On the whole, the observed picture agrees with the literature data^[16,19]. Displacements of relative positions of maxima of endo- and exo-peaks during the heating-cooling process (the hysteresis effect) can be an important indication of the nature of phase transitions^[30]. To be more exact, the effects of hysteresis should be observed for the transitions of the first order (structural transitions), while for the transitions of the second order they must be absent.

However^[30], it is known that experimental errors (displacements of peaks) associated with the effect of thermo resistance, that strongly depends on the mass of the sample and scanning velocity, can occur in DSC studies.

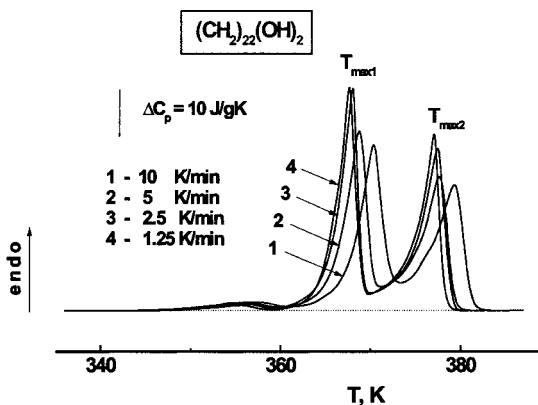


Figure 4. DSC thermographs of 1,22 – Docosanediol recorded at various scan rate.

As an example, Figure 4 shows thermograms of the D-22 sample obtained when the heating rate was varied from $1.25 \text{ K} \cdot \text{min}^{-1}$ to $10 \text{ K} \cdot \text{min}^{-1}$. It can be seen that not only do the positions of the

peaks at $T_{\max 1}$ and $T_{\max 2}$ shift by several degrees, but also the important characteristic of the half widths of the maxima changes considerably.

Illers showed^[31] that experimental errors can be eliminated. To this end, from the experimental data obtained for a wide range of heating rates V , the $T_{\max(\text{exp})} = f(V^{1/2})$ dependencies, which must be linear in the case of absence of any phase transitions, are plotted. Extrapolation of the linear dependencies to $V \rightarrow 0$ yields the true transition temperatures.

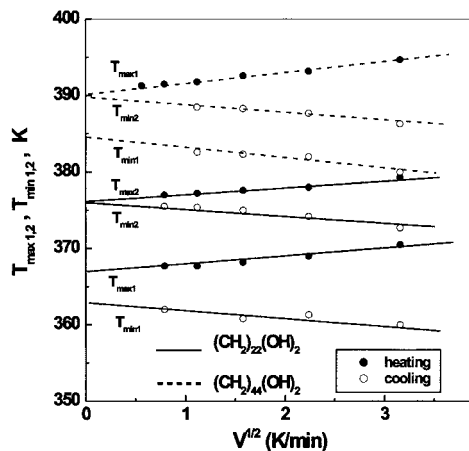


Figure 5. Dependence of phase transition temperatures on scan rate for 1,22 – Docosanediol and 1,44 – Tetratetracontanediol.

Figure 5 shows the $T_{\max(\text{exp})} = f(V^{1/2})$ dependencies for the D-22 and D-44 samples in the heating-cooling cycles. Table 1 gives extrapolated (true) phase transition temperatures $T_{\max 1}$ and $T_{\min 1}$, and also $T_{\max 2}$ and $T_{\min 2}$.

The data given in Figure 5 and Table 1 indicate that there is no hysteresis for positions of second maxima for D-22 and D-44 in the heating-cooling cycles. In accordance with the theories of phase transition,^[30] these DSC data lead to the conclusion that the high-temperature transition in the diols studied is indeed the second-order transition of the order-disorder type, and the hysteresis observed earlier in a number of studies in heating-cooling cycles was due to experimental inaccuracies.

Table 1. True thermodynamical parameters of phase transition in 1,22 – Docosanediol and 1,44 – Teteratetracosanediol.

Sample	$T_{\max 1}^r$	$T_{\max 2}^r$	$T_{\min 1}^r$	$T_{\min 2}^r$	ΔT_1	ΔT_2	ΔH_1	ΔH_2	ΔS_{\exp} 1	ΔS_{\exp} 2
	K	K	K	K	K	K	J/g	J/g	J/gK	J/gK
C ₂₂ (OH) ₂	367.1	376.3	362.8	376.3	4.3	0	108.6	151.4	–	0.407
C ₄₄ (OH) ₂	–	390.0	384.0	390.0	6.0	0	–	288.7	–	0.740

On the other hand, a pronounced hysteresis is observed for the low-temperature transition, even for extrapolated temperatures at $V \rightarrow 0$, which can be an additional argument showing that this transition is of the first order, i.e., the structural transition associated typically with the change of the crystallographic subcell type (see below).

Additional information on the nature of observed phase transitions can also be obtained from analysis of the shape of peaks on the thermograms of the samples studied.

It has been shown^[32] that, for the first-order transition, the endothermal peak must be δ -like shaped and have hysteresis in the heating-cooling cycle.

On the other hand, characteristic features of the transition of the order-disorder type (of the second order) is a λ -like shape of the $C_p(T)$ peak and the absence of hysteresis in the heating-cooling cycle.^[33] Figure 6 demonstrates for D-22, as an example, that these requirements for the peak shapes are fulfilled when each of the maxima (Figure 6b and c) is separated out from the complicated thermogram (Figure 6a).

It has also been shown^[30] that at temperatures $T < T_{\max 2}$ the $C_p(T)$ dependence is described by the power function of the type

$$p(T) = A + B(T_0 - T)^{-n}, \quad (1)$$

where A, B, T_0 , and n are constants. T_0 has the meaning of the true temperature of the second-order phase transition.

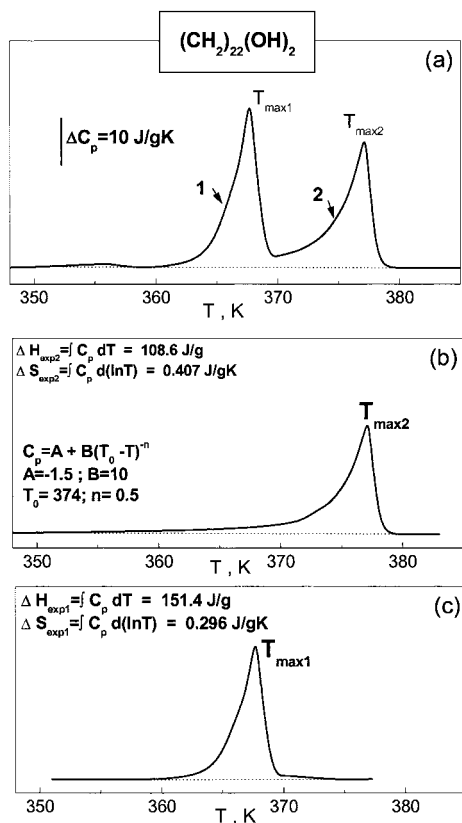


Figure 6. Deconvolution of experimental DSC endo thermogram of 1,22 – Docosanediol (a) into two peaks corresponding T_{max2} – order-disorder transition (b) and T_{max1} – solid-solid transition T_{ss} (c).

For the experimental $C_p(T)$ dependence of D-22, a good agreement between calculated and experimental curves was obtained if fitting parameters $A = 1.5$, $B = 10$, $n = 0.5$, and $T_0 = 374 \text{ K}$

were used.

Note that the obtained $T_0 = 374$ K differs from the value given in Table 1 ($T_{\max 2} = 376.3$ K). The reasons for this discrepancy are unclear at present.

It is believed^[30, 33, 34] that the abnormal change in heat capacity at the order-disorder transition is due to a change in the conformational entropy, whose limiting value at the crystal-melt transition is^[34]

$$S_c = R \cdot \ln 2 = 5.73 \text{ J} \cdot \text{mol}^{-1} \cdot \text{K}^{-1} \quad (2)$$

The experimental value of ΔS_c determined from

$$\Delta S_{\text{exp}}^{\max 2} = \int C_p(T) d(\ln T) \quad (3)$$

turned out to be

$$\Delta S_{\text{exp}}^{\max 2} = 0.407 \text{ Jg}^{-1} \text{K}^{-1} \quad (4)$$

Comparison of Equation (2) and Equation (4) yields the value of “mole” in our case

$$\Delta S_{\text{exp}}^{\max 2} = 0.407 \text{ Jg}^{-1} \text{K}^{-1} \equiv \Delta S_c = 5.73 \text{ J} \cdot \text{mol}^{-1} \text{K}^{-1}$$

i.e.,

$$1 \text{ mole} = 14.08 \text{ g},$$

which corresponds to the mol mass of the CH_2 group. This is consistent with the statement that the main role in realization of the second-order transition is played by kinetic units consisting of CH_2 groups.

Associated with this, it is interesting to find what contribution to this transition comes from end hydroxyl groups which, by forming a network of hydrogen bonds on the surfaces of elementary

lamellae, prevent mobility under unfreezing. In particular, they considerably increase the melting temperature of diols compared with n-paraffins with the same number of carbon atoms in the chain.

Let us consider the entropy of a system consisting of two basic constituents - CH₂ groups and CH₂OH groups. For such a system, the entropy is

$$\Delta S_c = (n_1 + n_2) R \cdot \ln 2 = (N_1/M_d + N_2/M_d \cdot \frac{1}{K}) R \cdot \ln 2 = 5.73 \text{ J} \cdot \text{mol}^{-1} \text{ K}^{-1},$$

where N_1 is the number of moles of CH₂ groups in one mole of diol ($N_1 = 20$ for D-22); N_2 is the number of moles of CH₂OH groups in one mole of diol ($N_2 = 2$ for D-22).

$$K = \frac{M_{\text{CH}_2}}{M_{\text{CH}_2\text{OH}}} ; \quad M_{\text{CH}_2} = 14; \quad M_{\text{CH}_2\text{OH}} = 31$$

$$M_{\text{D-22}} = 342; \quad K = \frac{14}{31} \cong 0.452$$

$$n_1 = \frac{N_1}{M_d} = \frac{20}{342} = 0.0585 \text{ mol/g}$$

$$n_2 = \frac{N_2}{M_d} \cdot \frac{1}{K} = \frac{2}{342 \cdot 0.452} = 0.0129 \text{ mol/g}$$

Then

$$\Delta S_c \cong (0.0585 + 0.0129) \cdot 5.37 \text{ J} \cdot \text{mol}^{-1} \text{ K}^{-1} = 0.409 \text{ J} \cdot \text{mol}^{-1} \text{ K}^{-1} \approx \Delta S_{\text{exp2}} = 0.407 \text{ J} \cdot \text{mol}^{-1} \text{ K}^{-1}.$$

Thus, our model is in good agreement with experimental data and allows estimation of the relative contributions of CH₂ and CH₂OH groups into the entropy of the order-disorder transition as

$$W = 0.129/0.0585 \cong 0.22 \cong 22 \%$$

These estimates show that despite a relatively low (~10 %) mole fraction of CH₂OH end groups in the molecule of D-22, their contribution to a change of entropy at the order-disorder transition

is fairly large, i.e., about 22 %.

As noted above, the low-temperature (structural) first-order transition is typically attributed to the change in the type of packing of molecules in subcells of crystalline lamellae accompanied by conversion of subcells with lower symmetry into subcells with symmetry of a higher order. In the literature on X-ray structural analysis of diols^[17, 18], data on parameters of subcells are generally not, though it is supposed that packing of methylene sequences at low temperatures is orthorhombic and the subcell parameters of diols are similar to those of n-paraffins and polyethylene^[35], i.e., $a_s = 7.4$ Å, $b_s = 4.96$ Å, and $c_s = 2.54$ Å. It is also believed^[36] that the first-order transition is accompanied by transformation of the orthorhombic elementary subcells into hexagonal (rotational) subcells.

Valuable information on the type of subcells and character of structural transformations at phase transitions in D-22 and D-44 can be obtained from analysis of IR spectroscopic data.

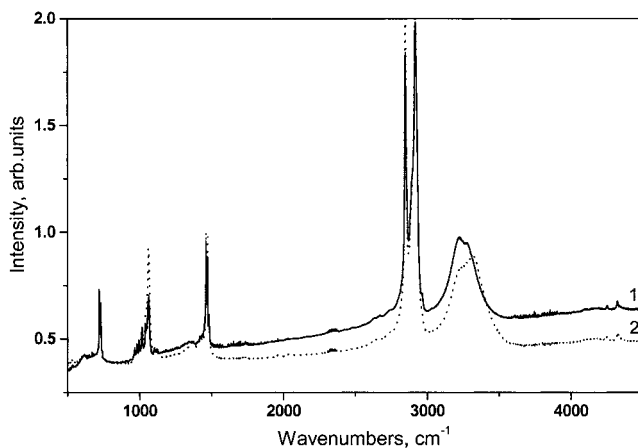


Figure 7. FTIR spectra of 1,22 – Docosanediol (1) and 1,44 – Tetratetracontanediol (2).

Figure 7 shows IR Fourier spectra in the frequency range from 500 cm^{-1} to 4500 cm^{-1} for D-22 (curve 1) and D-44 (curve 2). The spectra are seen to have intense characteristic absorption bands,

typical of crystals consisting of methylene sequences with orthorhombic subcells, i.e., well known doublets of methylene rocking mode bands at $720\text{--}730\text{ cm}^{-1}$, methylene bending mode bands at $1463\text{--}1473\text{ cm}^{-1}$, and symmetric and asymmetric stretching C-H mode bands at $\nu_s = 2850\text{ cm}^{-1}$ and $\nu_a = 2917\text{ cm}^{-1}$ ^[37].

In addition to the bands caused by the methylene part of the molecules, the spectra exhibit a narrow band at $\nu = 1067\text{ cm}^{-1}$ and a very broad band in the region from 3000 cm^{-1} to 3600 cm^{-1} .

According to literature^[38], the band at $\nu = 1067\text{ cm}^{-1}$ corresponds to the C-O stretching mode of a hydroxyl group, and the broad band is due to the O-H stretching mode of the hydroxyl groups forming intermolecular polymer sequences consisting of hydrogen bonds of the (O-H...O) type (see below).

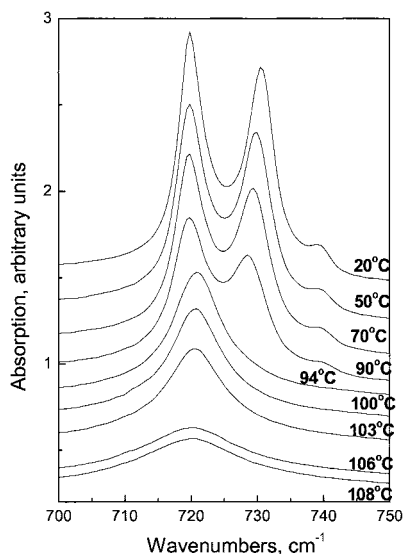


Figure 8. Temperature dependence of methylene rocking mode doublets in 1,22 – Docosanediol.

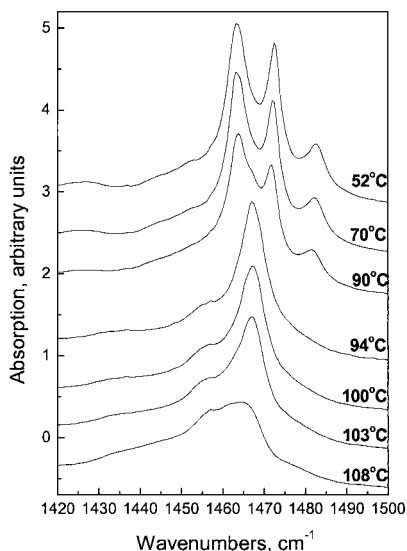


Figure 9. Temperature dependence of methylene bending mode doublets in 1,22 – Docosanediol.

Figures 8-11 show changes in the doublets at $720/730\text{ cm}^{-1}$ and $1463/1473\text{ cm}^{-1}$ as temperature is increased from room temperature to $T > T_m$ for D-22 and D-44. It is obvious from these figures that there are phase transformations in subcells.

The temperature changes in the doublets of diols are similar to the behavior of analogous doublets arising on heating of n-paraffins and polyethylene.

First of all, information on the change in the subcell type can be inferred from the behavior of the high-frequency components (730 cm^{-1} and 1473 cm^{-1}) of doublets. It is known^[39] that just the high-frequency component appears in IR spectra of hydrocarbons as factor group splitting resulting from specific intermolecular interactions between two chains in the orthorhombic subcell when the planes of trans-zigzags in neighboring layers of the molecules are perpendicular to each other. If this specific arrangement is disturbed (for example, in a hexagonal subcell), a single band ascribed to an isolated trans-zigzag is observed instead of a doublet.

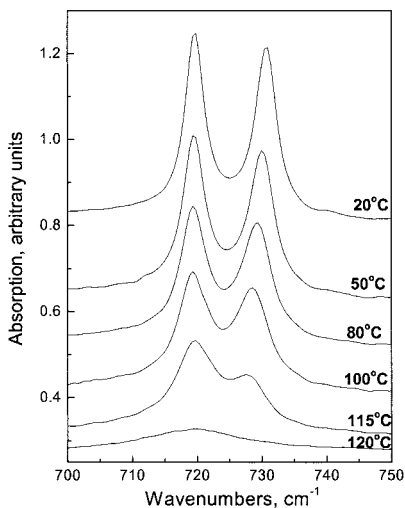


Figure 10. Temperature dependence of methylene rocking mode doublets in 1,44 – Tetratetracosanediol.

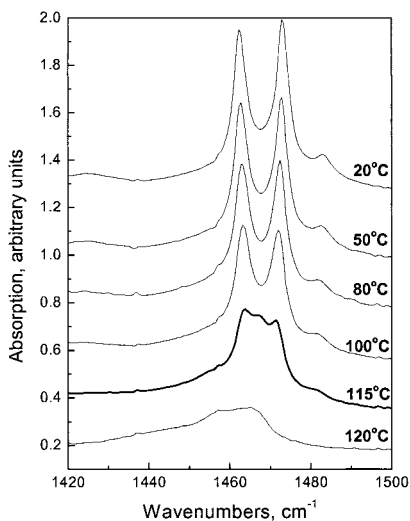


Figure 11. Temperature dependence of methylene bending mode doublets in 1,44 – Tetratetracosanediol.

It is known that the temperature-induced phase transition from the orthorhombic to hexagonal packing is accompanied by an increase in the volume of the initial ortho-subcell resulting from thermal expansion of a crystal. X-ray studies^[40] have shown that, on thermal expansion, parameter a of the subcell experiences larger changes than parameter b .

It has been shown^[39] that high-frequency components of doublets are polarized along the a parameter, while low-frequency components are polarized along the b parameter.

Therefore, it can be expected that the high-frequency components of doublets will be most sensitive to external factors, which was indeed observed in a number of studies of n-paraffins and polyethylene^[41, 42].

As follows from Figures 8-11, the high-frequency component in D-22 and D-44 is also most sensitive to temperature. Intensities of bands at 730 cm^{-1} and 1473 cm^{-1} gradually decrease, and eventually these bands vanish. The maxima of the high-frequency components shift toward lower frequencies by several cm^{-1} . The intensities of low-frequency components also gradually decrease, and their maxima shift toward higher frequencies.

Since both doublets consist of overlapping bands, correct quantitative estimates of changes in intensities, half widths of bands and frequency shifts of maxima can be obtained by using computer fitting of the doublets. These investigations are in progress, and detailed results are to be published.

It can be seen from Figures 8-9 that, at the temperature of solid-state phase transition $T_{s-s} = T_{\max 1} = 94\text{ }^{\circ}\text{C}$, splitting of both doublets for D-22 disappears, and, instead, single broad bands with maxima at 720.9 cm^{-1} and 1467.3 cm^{-1} arise. As the melting temperature $T_{\max 2} = 103\text{ }^{\circ}\text{C}$ is approached, a weak decrease in the frequencies of maxima (720.4 cm^{-1} and 1467.0 cm^{-1}) is observed. This tendency is preserved at $T > T_{\max 2}$.

It should be noted that the band at 1467 cm^{-1} of D-22 is asymmetric on the low-frequency side already when it arises at $T = T_{s-s} = 94\text{ }^{\circ}\text{C}$ (Figure 9). This indicates that this band consists of several overlapping bands. As temperature is increased, especially to $T > T_m$, asymmetry

continues to increase. Detailed analysis of this complicated profile is currently being carried out, and the results will be published elsewhere.

For D-44 in the heating cycle, DSC (Figure 3) has revealed only the order-disorder transition (melting) at true $T_m = 117\text{ }^{\circ}\text{C}$. FTIR spectroscopic data (Figure 10) show that up to $T \cong 118\text{ }^{\circ}\text{C}$ the band faintly resembling a doublet is observed at $719.6\text{ cm}^{-1}/727\text{ cm}^{-1}$. But at $T = 120\text{ }^{\circ}\text{C}$ (true $T_m + 3\text{ K}$) it becomes a broad band with a maximum at about $\nu = 719.7\text{ cm}^{-1}$. At higher temperatures ($130\text{ }^{\circ}\text{C}$), an extremely wide band with a maximum at $\nu = 719.5\text{ cm}^{-1}$ is seen.

Of interest is the behavior of the doublet at $1463.7/1471.1\text{ cm}^{-1}$ in D-44 (Figure 11). At $T = 115\text{ }^{\circ}\text{C}$, i.e., below T_m , a third peak at $\nu = 1466.6\text{ cm}^{-1}$ appears, in addition to the doublet. It has nearly the same intensity and corresponds to the CH_2 bending mode band of an isolated trans-zigzag.

This result is rather important because it indicates that the regions with the low-temperature orthorhombic subcells and regions with the hexagonal subcells co-exist in D-44 below T_m . It is likely that phase transition does not occur simultaneously throughout the entire lamellar volume; a new phase arises in the form of separate domains in the volume of the old phase.

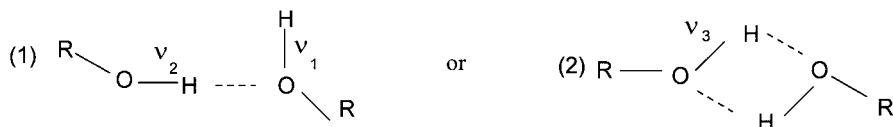
As temperature is further increased to $T = 120\text{ }^{\circ}\text{C}$, the doublet disappears, and only a single strongly anisotropic band (on the low-frequency side) is observed. It requires computer fitting, as the band for D-22.

The frequencies at the maxima of single bands (at $\nu \cong 720\text{ cm}^{-1}$ and $\nu \cong 1467\text{ cm}^{-1}$) are typical of hexagonal molecular packing of n-paraffins^[42]. As known^[36], a considerable weakening of the intermolecular interaction occurs at the ortho-hexagonal phase transition due to an increase in the subcell volume. As temperature increases, molecules get sufficient energy to oscillate, twist or rotate about their two-fold screw axes, to such an extent that their cross sections become statistically circular. The basal ab-plane expands so as to make the packing of the chains equal to closest packing of circular rods, i.e., hexagonal subcell.

Of particular interest is analysis of the behavior of absorption bands associated with end hydroxyl

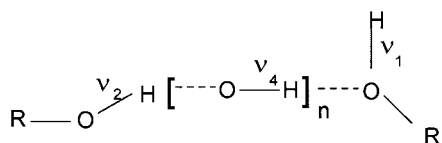
groups. In this paper, we analyze only the broad band in the region from 3000 cm^{-1} to 3600 cm^{-1} , which is due to absorption of the O-H stretching vibration of hydroxyl groups. The behavior of other bands and, in particular, the band at $\nu = 1067\text{ cm}^{-1}$ (C-O stretching mode) will be analyzed in a separate paper.

It has been shown^[43] that for single (monomer) hydroxyl groups, the O-H stretching mode manifests itself in the form of a very narrow band at $\nu_0 \cong 3650\text{ cm}^{-1}$. Single-bridge dimers (1) or double-bridge dimers (2) can arise if hydrogen bonds of the type



are formed. In this case, the (O-H) bond participating in formation of the hydrogen bond becomes weaker, which gives rise to absorption bands at $\nu_1 = 3623\text{ cm}^{-1}$, $\nu_2 = 3496\text{ cm}^{-1}$, and ν_3 between 3623 cm^{-1} and 3378 cm^{-1} .

When polymer chains consisting of hydrogen bonds of the type



are formed, the most appreciable weakening of the (O-H) bond in the polymer sequence occurs: the frequency decreases to ν_4 , which can differ from ν_0 by several hundred cm^{-1} ^[38]. The change $\Delta\nu$ of vibration frequencies of (O-H) bonds is proportional to the change in the energy of hydrogen bonds when the distance between diol molecules varies.

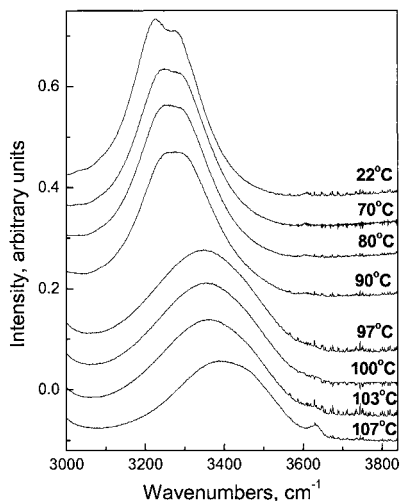


Figure 12. FTIR spectra of the O-H stretching mode of hydroxyl end groups in 1,22 - Docosanediol.

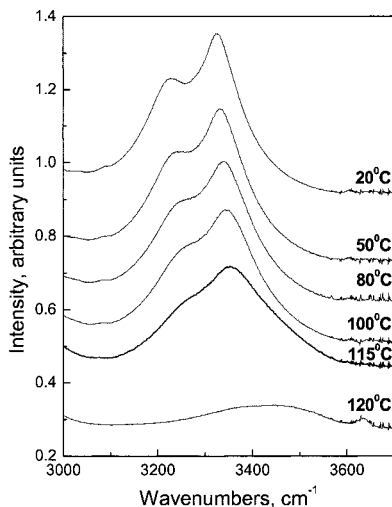


Figure 13. FTIR spectra of the O-H stretching mode of hydroxyl end groups in 1,44 - Tetratetracosanediol at different temperatures.

At room temperature, the absorption spectra of D-22 and D-44 shown in Figure 12 and Figure 13 have two pronounced broad overlapping bands with frequencies of the maxima

$$\text{D-22: } \nu \cong 3225 \text{ cm}^{-1} \text{ and } \nu \cong 3275 \text{ cm}^{-1}$$

$$\text{D-44: } \nu \cong 3225 \text{ cm}^{-1} \text{ and } \nu \cong 3325 \text{ cm}^{-1}$$

in the region from 3000 cm^{-1} to 3600 cm^{-1} . These frequencies differ considerably from $\nu \cong 3650 \text{ cm}^{-1}$ for a monomer and, no doubt, are the evidence of formation of polymer sequences consisting of hydrogen bonds on lamellar surfaces. We suppose that the presence of two maxima with

different frequencies is due to formation of polymers sequences in different crystallographic directions of the orthorhombic subcell.

As temperature is increased, the spectrum of D-22 (Figure 12) undergoes appreciable changes well below the phase transition temperature $T_{s-s} = 94\text{ }^{\circ}\text{C}$: two bands gradually merge into one broad band and its maximum shifts toward higher frequencies. These effects point to weakening and averaging of the strength of hydrogen bonds, which is, evidently, caused by thermal expansion of the ortho-subcell. This suggests that the frequency $\nu = 3225\text{ cm}^{-1}$ in D-22 is attributable to polymer chains consisting of hydrogen bonds formed along the a parameter of the orthorhombic subcell.

Changes at $T > T_{s-s}$ are even more appreciable: at $T = 97\text{ }^{\circ}\text{C}$ there is only a single very wide band with the maximum at about $\nu \cong 3350\text{ cm}^{-1}$ (D-22 has hexagonal subcells). On further heating ($T = 107\text{ }^{\circ}\text{C} > T_m$), the band half width becomes even wider, and the maximum shifts to $\nu \cong 3400\text{ cm}^{-1}$. However, this frequency still differs significantly from $\nu \cong 3650\text{ cm}^{-1}$ for a monomer.

Thus, in spite of transition of D-22 into the melt, and, hence, a higher molecular mobility, end hydroxyl groups of the molecules turn out to be linked by hydrogen bonds. Note that a pronounced single band at $\nu \cong 3630\text{ cm}^{-1}$ appears in the spectrum of the melt. According to^[43], vibrations with frequencies $\nu \cong 3350\text{ cm}^{-1} \div 3500\text{ cm}^{-1}$ and $\nu \cong 3630\text{ cm}^{-1}$ indicate that the melt can contain agglomerates of molecules of diols linked by single-bridge or double-bridge dimers.

The spectra of D-44 (Figure 13) at room temperature also exhibit two rather wide overlapping bands with $\nu \cong 3225\text{ cm}^{-1}$ and $\nu \cong 3325\text{ cm}^{-1}$, which indicate, like for D-22, that polymer chains consisting of hydrogen bonds are formed. In contrast to D-22, heating of D-44 does not give rise to a phase T_{s-s} transition of the ortho-hexagonal subcell type, and, therefore, two wide absorption bands are observed up to $T \cong T_m$. This is an additional proof of a higher stability of orthorhombic crystals in D-44, the methylene sequences in which are twice as long as those in D-22. At $T > T_m$ ($120\text{ }^{\circ}\text{C}$ and $130\text{ }^{\circ}\text{C}$), only a single extremely wide band with the maximum in the vicinity of $\nu \cong 3430\text{ cm}^{-1}$ is detected. At these temperatures the single band at $\nu \cong 3635\text{ cm}^{-1}$ becomes more and more pronounced (like in D-22). Hence, similar to D-22, single-bridge or double-bridge dimers

are formed between neighboring diol molecules in the melt of D-44 (with participation of hydrogen bonds).

Conclusions

Similarly to other long-chain molecular crystals, α,ω -alkanediols $(\text{CH}_2)_{22}\text{OH}$ and $(\text{CH}_2)_{44}(\text{OH})_2$ exhibit a well developed morphology, characterized by the presence of large stacks of superposed crystalline lamellae with the thickness proportional to the molecule length.

Splitting of the IR absorption bands into doublets at $720\text{--}730\text{ cm}^{-1}$ and $1463\text{--}1473\text{ cm}^{-1}$ indicates that crystalline subcells in the lamellae of both diols are of the orthorhombic type, with the parameters typical of hydrocarbons.

Analysis of the DSC data obtained in experiments where the heating rate was varied from $V = 1.25\text{ K}\cdot\text{min}^{-1}$ to $V = 10\text{ K}\cdot\text{min}^{-1}$ allowed estimation of the true solid-state transition temperatures for $(\text{CH}_2)_{22}(\text{OH})_2$ ($T_{s-s} = 367.1\text{ K}$) and melting temperatures (order-disorder transition) for $(\text{CH}_2)_{22}(\text{OH})_2$ ($T_m = 376.3\text{ K}$) and $(\text{CH}_2)_{44}(\text{OH})_2$ ($T_m = 390.0\text{ K}$). It has been shown that hysteresis of T_m in the heating-cooling cycles observed in a number of studies was caused by experimental inaccuracies.

Upon heating of $(\text{CH}_2)_{22}(\text{OH})_2$ in the range $T_{s-s} < T < T_m$, splitting of the IR bands at $720\text{--}730\text{ cm}^{-1}$ and $1463\text{--}1473\text{ cm}^{-1}$ disappears and, instead, only single bands are observed. This indicates that transformation of the orthorhombic subcell into a hexagonal one occurs at the phase transition temperature (T_{s-s}). This type of molecular chain packing remains the same up to the melting temperature T_m .

In a $(\text{CH}_2)_{44}(\text{OH})_2$ diol, the ortho-hexagonal subcell transition occurs only at the melting temperature (390.0 K).

Analysis of the wide IR absorption band in the region from 3000 cm^{-1} to 3600 cm^{-1} has led to the conclusion that end hydroxyl groups of diol molecules form on the surfaces of lamellar crystals long (polymer) regular sequences consisting of intermolecular hydrogen bonds. These sequences

are arranged in different crystallographic directions.

Linking of the ends of diol molecules by hydrogen bonds becomes weaker on heating, but it is preserved even in the melt. In the melt, single-bridge or double-bridge dimers are formed between neighboring diol molecules (with participation of hydrogen bonds).

Acknowledgements

The authors would like to acknowledge financial support of the Russian Foundation for Basic Research (grant No. 01-03-32773).

- [1] J. D. Hoffmann, B. F. Decker, *J. Phys. Chem.* **1953**, 57, 520.
- [2] M. G. Broadhurst, *J. Res. Nat. Bur. Stands, A, Phys. and Chem.* **1962**, 66A, 241.
- [3] P. K. Sullivan, *J. Res. Nat. Bur. Stands, A, Phys. and Chem.* **1974**, 78A, 129.
- [4] V. Daniel, *Phil. Mag, Suppl.* **1953**, 450.
- [5] P. J. Flory, A. Vrij, *J. Am. Chem. Soc.* **1963**, 85, 3548.
- [6] M. F. Mina, T. Asano, T. Takahashi, I. Hatta, K. Ito, Y. Amemiya, *Jpn. J. Appl. Phys.* **1997**, 36, pt.1, 5616.
- [7] J. Techoe, D. C. Bassett, *Polymer* **2000**, 41, 1953.
- [8] G. Strobl, B. Ewen, E. W. Fischer, W. Piesczek, *J. Chem. Phys.* **1974**, 61, 5257; *J. Chem. Phys.* **1974**, 61, 5265. [9] G. R. Strobl, *J. Polym. Sci., Polym. Symp.* **1977**, 59, 121.
- [10] H. L. Casal, D. G. Cameron, H. H. Mantsch, *Can. J. Chem.* **1983**, 61, 1736.
- [11] C. Chang, S. Krimm, *J. Polym. Sci., Polym. Phys. Ed.* **1979**, 17, 2163.
- [12] G. Ungar, N. Masic, *J. Phys. Chem.* **1985**, 89, 1036.
- [13] G. Ungar, *J. Phys. Chem.* **1983**, 87, 689.
- [14] A. S. Vaughan, G. Ungar, D. C. Bassett, A. Keller, *Polymer* **1985**, 26, 726.
- [15] T. Asano, M. F. Mina, I. Hatta, *J. Phys. Soc. Japan* **1996**, 65, 1699.
- [16] H. Kabayashi, N. Nakamura, *Cryst. Res. Technol.* **1995**, 30, 495.
- [17] N. Nakamura, S. Setodoi, *Acta Cryst.* **1997**, C53, 1883.
- [18] N. Nakamura, T. Yamamoto, *Acta Cryst.* **1994**, C50, 946.
- [19] Y. Ogawa, N. Nakamura, *Bull. Chem. Soc. Jpn.* **1999**, 72, 943.
- [20] R. Popovitz-Biro, J. Majewski, L. Margulis, S. Cohen, L. Leiserowitz, M. Lahav, *J. Phys. Chem.* **1994**, 98, 4970.
- [21] D. M. Small, "The Physical Chemistry of Lipids", Plenum, N.Y.-London 1986.
- [22] C. Le Fevere de Ten Hove, A. Jonas, J. Penelle, *Proc. Am. Chem. Soc. Div. Polym. Mater. Sci. Eng.* **1997**, 76, 158.
- [23] E. E. Rusanova, Y. L. Sebyakin, L. V. Volkova, R. P. Evstigneeva, *J. Org. Chem. USSR*, **1984**, 20, 248.
- [24] B. G. Ranby, F. F. Morehead, N. M. Walter, *J. Polym. Sci.* **1960**, 44, 349.
- [25] A. Keller, *Phil. Mag.* **1961**, 6, 329.
- [26] H. Zocher, R. D. Machado, *Acta Cryst.* **1959**, 12, 122.
- [27] I. M. Dawson, V. Vand, *Proc. Royal Soc., London, Ser. A.* **1951**, 206A, 555.
- [28] S. Amelinckx, *Acta Cryst.* **1956**, 9, 217.
- [29] I. M. Dawson, *Proc. Royal Soc. London*, **1952**, A214, 72.
- [30] L. D. Landau, E. M. Liphshitz, "Statistical Physics", Nauka, Moscow 1976, Ch. XIV.

- [31] V. A. Bershtein, V. M. Egorov, *"Differential Scanning Calorimetry of Polymers: Physics, Chemistry, Analysis, Technology"*, Ellis Horwood, N.Y., 1994.
- [32] J. Sestak, *"Thermophysical Properties of Solids"*, Academia, Prague 1984.
- [33] M. Fisher, *"Nature of critical state"*, Mir, Moscow 1973.
- [34] L. A. Nikolaev, V. A. Tulupov, *"Physical Chemistry"*, Khimiya, Moscow 1967.
- [35] C. W. Bunn, *Trans. Far. Soc.* **1939**, 35, 482.
- [36] A. Mueller, *Proc. Roy. Soc.* **1932**, 138, 514.
- [37] S. Krimm, *Adv. Polym. Sci.* **1960**, 2, 51.
- [38] K. Nakamishi, *"Infrared Absorption Spectroscopy"*, Holden-Day, San Francisco 1962, Ch.II.
- [39] R. G. Snyder, *J. Mol. Spect.* **1961**, 7, 116.
- [40] G. T. Davis, R. K. Eby, G. M. Martin, *J. Appl. Phys.* **1968**, 39, 4973.
- [41] H. L. Casal, H. H. Mantsch, D. G. Cameron, R. G. Snyder, *J. Chem. Phys.* **1982**, 77, 2826.
- [42] J. R. Nielsen, C. E. Hathaway, *J. Mol. Spectr.* **1963**, 10, 366.
- [43] F. A. Smith, E. C. Creitz, *J. Res. Nat. Bur. Stands.* **1951**, 46, 145.